

# Deposition kinetics of nanocolloidal gold particles

E.A. Martijn Brouwer, E. Stefan Kooij\*, Mark Hakbijl,  
Herbert Wormeester, Bene Poelsema

MESA+, Institute for Nanotechnology, University of Twente, P.O. Box 217, 7500 AE Enschede, The Netherlands

Available online 2 August 2005

## Abstract

The deposition kinetics of the irreversible adsorption of citrate-stabilized, nanocolloidal gold particles on Si/SiO<sub>2</sub> surfaces, derivatized with (aminopropyl)triethoxysilane (APTES), is investigated in situ using single wavelength optical reflectometry. A well-defined flow of colloids towards the surface is realized using a radial impinging jet cell geometry. The dynamics of the deposition process is at first mass transport limited. Surface blocking effects determine the adsorption kinetics in the final stage. The entire deposition process can be adequately described in terms of a generalized adsorption theory, which combines the effects of mass-transport and the actual adsorption onto the surface. The diffusion coefficient of the particles is calculated from the initial deposition rate. The obtained value corresponds well with data obtained from experiments described in literature and with the value calculated from the Stokes–Einstein relation.

© 2005 Elsevier B.V. All rights reserved.

**Keywords:** Nanocolloidal gold particles; Deposition kinetics; Ionic strength; RSA

## 1. Introduction

The deposition kinetics of colloidal particles are influenced by many factors. Obviously, particle size, shape and polydispersity as well as surface heterogeneities are important. But also electrostatic and/or steric particle–particle interactions, particle–substrate interactions, forced convection and the presence of external fields (shear, electric, magnetic) can have a profound effect on the adsorption process and the resulting distribution of particles on the surface. Both reversible and irreversible deposition of a large number of colloidal systems have been investigated, but the scope is primarily limited to relatively large particles, which can be directly observed by optical microscopy.

For particles with dimensions well below the diffraction limit of (visible) light, such as proteins [1] or nanocolloidal particles [2,3], it is difficult to monitor the deposition process in a truly in situ manner. Obviously, analysis can be done after deposition using many techniques, e.g. electron microscopy (SEM/TEM) or scanning probe microscopy (STM, AFM), but the influence of drying effects and reorientation upon

change of ambient may hinder proper analysis in terms of real deposition parameters.

In this paper, we study the irreversible deposition characteristics of colloidal particles with dimensions in the low-nanometer range using optical reflectometry in a stagnation point flow geometry<sup>1</sup> [4]. As mentioned above, considerable effort has been devoted to (irreversible) deposition of micrometer sized particles. For these large particles the RSA model adequately describes the overall deposition kinetics. However, for considerably smaller particles in the 10–100 nm range, this relatively simple model fails to describe the deposition kinetics, although it gives a good description of the particle distribution after saturation of the adsorption process [5]. Böhmer et al. [6] presented a detailed study of the deposition kinetics of such small particles. The initial deposition rate as well as the characteristics in the saturation regime were in agreement with the RSA model. However, they were unable to quantitatively analyze their results over the entire coverage range. Recently we showed that the generalized adsorption model, as described in detail by Adamczyk [7–11], can describe deposition transients of particles in the low-nanometer

\* Corresponding author. Tel.: +31 53 489 3146; fax: +31 53 489 1101.  
E-mail address: [e.s.kooij@tnw.utwente.nl](mailto:e.s.kooij@tnw.utwente.nl) (E.S. Kooij).

<sup>1</sup> In many publications, this setup is also referred to as a radial impinging jet cell.

range over the entire coverage range [12], but experimental errors resulted in an inaccurate determination of the adsorption rate. In this paper, more accurate results are presented. Also, quantitative analysis of our results indicates that the adsorption rate, which strongly depends on particle size, is in good agreement with results of similar experiments using particles of very different nature [9] (i.e. various proteins) but roughly of the same size.

## 2. Experimental

Gold colloids are prepared by reduction of 250 ml 1 mM HAuCl<sub>4</sub> solution (Aldrich) with 25 ml 38.8 mM tri-sodium citrate (Aldrich) at 100 °C. The resulting colloids have an average radius of 6.7 nm with an 8% spread [5]. Based on the initial AuCl<sub>4</sub><sup>-</sup> ion concentration, and the average particle size, we estimate that the suspension contains approximately  $7.4 \times 10^{18}$  particles/m<sup>-3</sup>. Calculations of the absorbance using this concentration yield results which are in good quantitative agreement with UV–vis measurements [3]. Additionally, the suspension has an ionic strength of approximately 14.3 mM. Sodium chloride (Merck) is used to vary the ionic strength of the solution. Silicon substrates with a well-defined oxide thickness are cleaned ultrasonically in water and derivatized for 30 min in a 10% solution of 3-aminopropyltriethoxysilane (APTES, obtained from Merck) in methanol (Merck).

The stagnation point flow cell and the reflectometer are homebuilt at Philips Research [13]. The setup consists of a He–Ne laser, the stagnation point flow cell, a beamsplitter and two photodiodes for detection of the intensities  $I^p$  and  $I^s$  of the parallel and perpendicular components of the reflected light. A more extensive description of the setup is given by Dijt et al. [13]. The intensity ratio  $S \equiv I^p/I^s \equiv (I_0^p/I_0^s)(R^p/R^s)$  is measured, where  $I_0^p$  and  $I_0^s$  are the initial intensities and  $R^p$  and  $R^s$  are the intensity reflection coefficients. The polarization of the light source is eliminated by calculating  $Y \equiv (S/S_0) - 1$ , where  $S_0 = I_0^p/I_0^s$  is the value of  $S$  before deposition. The angle of the incident beam can be adjusted and is set to 70° with respect to the normal of the sample surface. The volume flow during the experiments was approximately 1.0 ml min<sup>-1</sup>.

For the reflectometry experiments, substrates cut from p-type silicon (100) wafers with a deposited oxide layer of 25 nm are used. When the oxide layer is too thin,  $R^p$  is very small and the initial sensitivity of the setup is low. With too thick oxide layers, the reflectometer signal flattens and even decreases above a certain surface concentration. This is shown in Fig. 1, where the reflectometer signal  $R^p/R^s$  is shown as a function of the surface coverage. These curves are calculated using the thin island film theory [3,14,15]. Details on the applied model and the calculation are presented elsewhere [3,14]. The figure shows that both for very thin and very thick oxides, single wavelength reflectometry has serious sensitivity problems. A similar curve calculated for

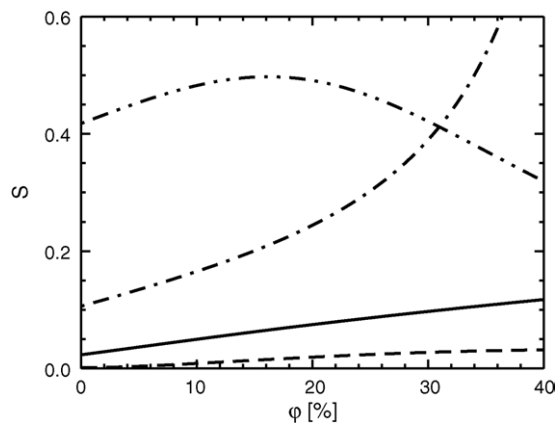


Fig. 1. Calculated reflectometry response (at 70° incident angle) as a function of the gold nanocrystal coverage for silicon substrates with oxide thicknesses of 2 nm (dashed line), 45 nm (solid line), 100 nm (dashed dotted line) and 200 nm (dashed dot dotted line).

an oxide film of 25 nm is used as calibration to convert the reflectometer signals to absolute surface coverages.

## 3. Results and discussion

In Fig. 2 typical reflectometry transients, obtained during colloidal gold deposition in the stagnation point flow cell at various ionic strengths, are shown. The coverage is defined as

$$\phi \equiv \pi a^2 \cdot N \quad (1)$$

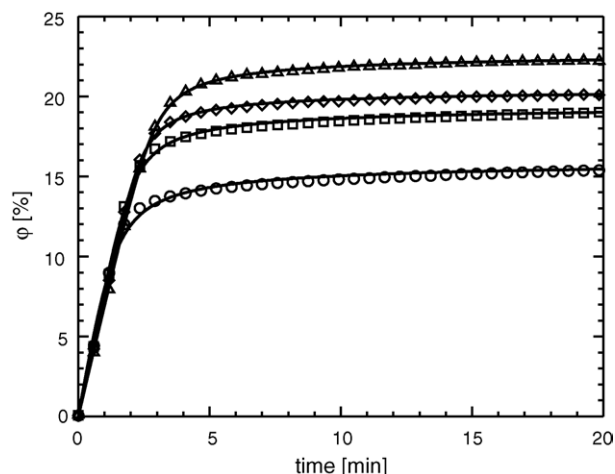


Fig. 2. Deposition of gold colloids on silicon with 25 nm oxide at different ionic strengths in a reflectometry experiment using the stagnation point flow geometry. The ionic strength is varied by adding NaCl. The ionic strengths of the solutions are 3.6 mM (circles), 6.1 mM (squares), 8.6 mM (diamonds) and 13.6 mM (triangles). The coverage is calculated from the reflectometer signal using the thin island film theory (see Fig. 1). The solid lines represent fits of the generalized adsorption model to the data, as will be described in the text.

where  $a$  is the particle diameter and  $N$  the number of particles per unit area. After dilution of the as-prepared colloidal gold suspension by a factor of 4, the particle number density amounts to  $1.85 \times 10^{18} \text{ m}^{-3}$ , while the minimum ionic strength is 3.6 mM. The ionic strength of the solution is varied by adding 0 to 10 mM NaCl, which corresponds to Debye screening lengths from 5.1 to 2.7 nm. For  $t < 0$  only water flows through the cell, and a constant base line is measured. At  $t = 0$  the gold suspension is injected in the cell. When the flow is switched back to water no noticeable decrease of the surface coverage is observed, indicating the absence of particle detachment. Two distinct regimes are observed in the measured curves in Fig. 2. At longer deposition times, the deposition process leads to a saturation at coverage values, which show a clear dependence on the ionic strength. The maximum coverage obtained in our experiments is equal to 22%, which is well below the limiting value of 54.8% for random deposition of hard spheres. The relatively low saturation coverage is caused by the thickness of the double layer that is comparable with the radius of the particles. A more extensive discussion on the saturation coverage is given elsewhere [12]. For short times the deposition rate is similar for all ionic strengths. This implies that initially the deposition process is limited by the supply of colloidal particles to the surface. We will use this later on to calculate the particle diffusion coefficient from the initial deposition rate.

The deposition kinetics of colloidal particles [8,9,11,16] can be described in terms of the adsorption rate  $d\varphi/dt$  by

$$\frac{d\varphi}{dt} = \pi a^2 \cdot j_0 \cdot B(\varphi) \quad (2)$$

where  $\pi a^2$  is the projected particle surface area and  $j_0$  represents the limiting deposition flux for uncovered surfaces. The quantity  $B(\varphi) = j(\varphi)/j_0$ , with  $j(\varphi)$  the actual deposition flux for a given coverage, is usually referred to as the overall kinetic blocking function [8,9,11,17]. In relation to our present results, this designation is somewhat misleading since  $B(\varphi) = 1$  for low coverages, while in the limit of saturating coverages  $B(\varphi) \rightarrow 0$ , so in fact  $B(\varphi)$  represents an effective, coverage dependent available surface. More correctly, it is also referred to as the ‘available surface function’. However, to be consistent with the work by Adamczyk, we will adopt the former designation of the blocking function. The function  $B(\varphi)$  not only depends on the coverage, but also on many additional factors such as particle–particle interactions, the mechanism of particle transport and the reversibility of particle adsorption.

A theory which is more specifically applicable to our system of colloidal particles, irreversibly deposited under forced convection (stagnation point flow geometry) conditions, has been extensively described by Adamczyk [8,9,11,18]. A similar model was also described by Faraudo and Bafaluy [19]. In this generalized adsorption model, the deposition is considered to consist of two processes as is schematically shown in Fig. 3. The adsorption process can be described by

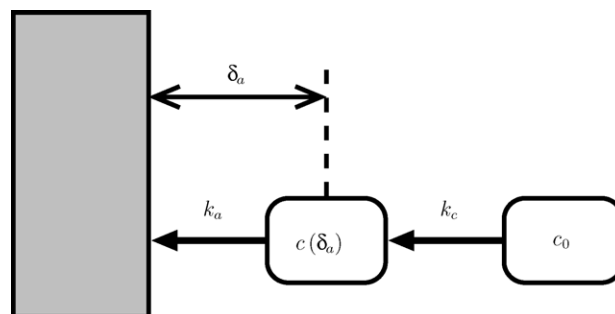


Fig. 3. Schematic representation of the deposition process, showing the two processes involved and the corresponding rate constants. Particles migrate from the bulk to the substrate. At a distance  $\delta_a$ , interactions between particles arriving at the substrate and adsorbed particles set in, resulting in an energy barrier that determines the adsorption constant  $k_a$ .

$$\frac{d\varphi}{dt} = \pi a^2 \cdot k_a c(\delta_a) \cdot \bar{B}(\varphi) \quad (3)$$

and is governed by a rate constant  $k_a$  and a particle concentration  $c(\delta_a)$  at distance  $\delta_a$  from the surface [7]. The available surface function  $\bar{B}(\varphi)$ , also often referred to as the generalized blocking function, describes the transport resistance of the adsorbed layer to adsorbing particles; effectively it is equal to the overall sticking probability. In fact, Eq. (3) is similar to Eq. (2). In Eq. (2), the actual adsorption process is taken into account by the overall kinetic blocking function  $B(\varphi)$  considering a constant supply of colloidal particles, while in Eq. (3) the adsorption process is considered and the supply of colloidal particles is described by the time-dependence of  $c(\delta_a)$ .

Within the adsorption layer of thickness  $\delta_a$ , particle–substrate interactions are playing a role. The thickness  $\delta_a$  is comparable to the range of the electrostatic interactions, the extent of which is governed by the double layer thickness. For our nanocolloidal particles, this implies that  $\delta_a$  is of the same order of magnitude as the particle radius. The adsorption rate constant  $k_a$  contains a barrier term in the particle–substrate interaction energy, which represents the repulsive electrostatic interaction of an adsorbing particle with the already adsorbed particles. The supply of colloidal particles to the outer edge of the adsorption layer, at a distance  $\delta_a$  from the surface, is described by the rate constant  $k_c = j_0/c_0$ , where  $j_0$  is equal to the particle flux [6–9,11]. When we assume a sticking probability of 1, the latter quantity can be obtained from the initial deposition rate.

For the irreversible adsorption of particles at uniformly accessible surfaces, Adamczyk derived an expression for the kinetic overall blocking function, given by [8,11]

$$B(\varphi) = \frac{K \bar{B}(\varphi)}{1 + (K - 1) \bar{B}(\varphi)} \quad (4)$$

where  $K = k_a/k_c$  represents the coupling between adsorption and diffusion processes. In the case of strong particle–particle interactions,  $\bar{B}(\varphi)$  can be approximated by the RSA available surface function  $B_0(\varphi)$  [8,11,17]. It is not possible

to evaluate  $B_0(\varphi)$  analytically, but a good approximation is given by [11,16]

$$B_0(\varphi) = \left( 1 + 0.812 \frac{\varphi}{\varphi_\infty} + 0.426 \left( \frac{\varphi}{\varphi_\infty} \right)^2 + 0.0716 \left( \frac{\varphi}{\varphi_\infty} \right)^3 \right) \left( 1 - \frac{\varphi}{\varphi_\infty} \right)^3 \quad (5)$$

With this expression the overall kinetic blocking function  $B(\varphi)$  can be calculated, using Eq. (4), which now only depends on the maximum coverage  $\varphi_\infty$  obtained after saturation and the coupling constant  $K$ .

In practice,  $K \sim 1$  for micrometer large particles [8,11]. However, our colloidal particles are markedly smaller, which leads to a significant increase of the value of  $K$ . This can be understood by considering the dependence of the diffusion coefficient and the adsorption constant  $k_a$  on the particle size. The Stokes–Einstein relation states

$$D = \frac{kT}{6\pi\eta a} \quad (6)$$

where  $kT$  is the thermal energy and  $\eta$  is the dynamic viscosity of the fluid (for water,  $\eta = 1.00 \times 10^{-3} \text{ kg m}^{-1} \text{ s}^{-1}$ ). When we model the repulsive interaction between the adsorbing particle and the particles present on the surface as an energy barrier with a parabolic potential distribution around the maximum  $\phi_b$ , the adsorption rate constant can be approximated by [8]

$$k_a = \frac{D}{a} \left( \frac{\phi_b}{\pi kT} \right)^{1/2} \exp \left( -\frac{\phi_b}{kT} \right) \quad (7)$$

This equation is only valid for large barrier heights. Another approach is to model the repulsive particle–particle interaction as a reduction of the diffusion coefficient of an adsorbing particle near the surface [20]. When there are no other contributions to the potential barrier, this yields

$$k_a = \frac{D}{2a} \frac{1}{1 + \frac{1}{2} \ln \left( 1 + \frac{\Delta a}{a} \right)} \quad (8)$$

where  $\Delta a$  represents the extent of the repulsive interactions, i.e. the effective thickness of the double layer. As shown later, the diffusive particle flux, expressed by the rate constant  $k_c$  varies as  $a^{-2/3}$ . Combining either Eqs. (7) and (8) with Eq. (6), we obtain for the coupling constant  $K = k_a/k_c \sim a^{-4/3}$ , i.e. for smaller particles  $K$  is expected to become considerably larger than 1.

In Fig. 4 the coverage dependence of the overall kinetic blocking function is plotted for different values of  $K$ . A large value of  $K (\gg 1)$  implies that the adsorption rate constant is considerably larger than the rate constant for diffusive transport of the particles. Thus, up to relatively large coverages the deposition is transport limited, which is expressed by the considerable  $\bar{\varphi}$ -range over which  $B(\bar{\varphi}) \approx 1$ . Only near the saturation coverage,  $B(\bar{\varphi})$  drops rapidly to 0. In the opposite

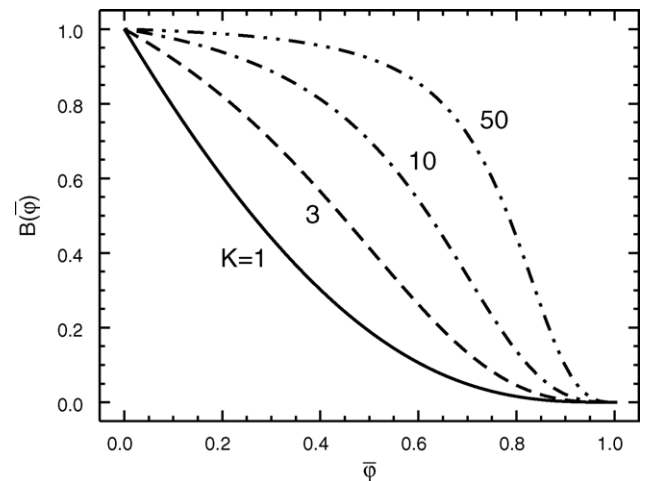


Fig. 4. The overall kinetic blocking function  $B(\bar{\varphi})$  for different values of the coupling constant  $K$  as function of the normalized coverage  $\bar{\varphi}$ . The solid line represents the RSA limit ( $K = 1$ ), the dashed, dash dotted and dash dot dotted lines correspond to calculations using  $K = 3, 10$  and  $50$ .

case when  $K \sim 1$ , corresponding to pure RSA, the adsorption itself becomes rate-limiting. Accordingly, for low  $K$  values,  $B(\bar{\varphi})$  exhibits a sharp decrease already at low coverages.

From the deposition curves in Fig. 2, it is obvious that for a large coverage range the deposition is dominated by mass transport of particles to the adsorption layer. The deposition rate  $d\varphi/dt$  only decreases upon approaching the saturation coverage. This indicates that for our system of nanocolloidal gold particles, irreversibly deposited in a stagnation point flow geometry,  $K$  is considerably larger than 1. To obtain more quantitative information, we fitted the generalized adsorption model, expressed by Eqs. (2), (4) and (5), to the deposition transients in Fig. 2. The saturation coverage  $\varphi_\infty$ , the coupling constant  $K$  and the initial deposition rate  $\pi a^2 j_0$  are used as fitting parameters. The results obtained by this fitting procedure are shown in Fig. 2 with lines. The resulting fit parameters are summarized in (Table 1). Over the entire coverage range there is a good correspondence between the measured and calculated deposition curves. The calculated initial deposition rate  $d\varphi/dt = \pi a^2 j_0$  amounts to  $0.080 \text{ min}^{-1}$ . Within the experimental error of about 9%, this value does not vary with ionic strength.

From the fits a coupling constant of  $K = 45 \pm 4$  is obtained. Using the value of  $k_c$  calculated using  $k_c = \frac{j_0}{c}$ , we obtain a value for the adsorption rate constant  $k_a = 2.1 \times 10^{-4} \text{ m s}^{-1}$ . Using Eq. (8) with  $\Delta a = 2 \text{ nm}$ , we obtain a value of  $k_a = 2.9 \times 10^{-4} \text{ m s}^{-1}$ , which is close to the experimentally determined value. Calculation of the adsorption barrier

Table 1  
Deposition parameters obtained from the fits shown in Fig. 2

$D (\mu \text{ m}^2 \text{ s}^{-1})$	44
$K$	$45 \pm 4$
$k_c (\text{m s}^{-1})$	$4.7 \times 10^{-6}$
$k_a (\text{m s}^{-1})$	$2.1 \times 10^{-4}$
$\phi_b (\text{kT})$	3.34

height  $\phi_b$  from the obtained adsorption rate constant, using Eq. (7) yields a value of  $3.34kT$  or  $84\text{ meV}$ . As far as we are aware, the absolute value of the adsorption rate constant  $k_a$  and adsorption barrier height  $\phi_b$  has not been determined for colloidal systems with particle sizes in the low nanometer range. However, Adamczyk [9] collected adsorption rate constants for typical proteins (BSA, fibrinogen and IgG), which are of the same order of magnitude as our colloidal particles. Comparison with the  $k_a$  values for these proteins<sup>2</sup> indicates that our aforementioned value for the irreversible deposition of nanocolloidal gold is in line with other systems of similar dimensions but of very different nature.

As stated previously, the initial deposition rate can be used to determine the diffusion coefficient of the colloids. The hydrodynamics of colloid deposition in a stagnation point flow cell have been discussed by Dabros and van de Ven [21] and also by Adamczyk et al. [4]. The initial particle flux towards the surface is in good approximation given by

$$j_0 = 0.776 \left( \frac{D^2 \bar{\alpha} \bar{V}_m}{R^2} \right)^{1/3} c_0 = k_c c_0 \quad (9)$$

where  $c_0$  is the bulk particle concentration,  $D$  is the diffusion coefficient of the nanocolloidal particles,  $R = 0.64\text{ mm}$  is the radius of the inlet tube and  $\bar{V}_m = \frac{v \cdot Re}{R}$  is the average flow velocity, with  $Re$  the Reynolds number and  $v$  the kinematic viscosity of the fluid. The dimensionless flow parameter  $\bar{\alpha}$  depends on the Reynolds number and the cell geometry parameter  $h/R$ . In our case, a value  $\bar{\alpha} = 4.2$  is obtained from the work of Dabros and van de Ven [21] using  $Re = 8.3$  and  $h/R = 1.7$ . Adamczyk et al. give an analytical expression for  $\bar{\alpha}$  for  $h/R = 1.6$ , from which a value of  $5.6$  is calculated [4].

Assuming a sticking probability of 1, the observed initial adsorption rate  $d\varphi/dt = \pi a^2 j_0 = 0.080\text{ min}^{-1}$  can be used to calculate the particle diffusion coefficient from Eq. (9). Inserting the known values for particle density and cell geometry parameters, we find  $D = 44\ \mu\text{m}^2\text{ s}^{-1}$ . We now compare this result to the diffusion coefficient obtained using the Stokes–Einstein relation. With a particle radius  $a = 6.7\text{ nm}$  the Stokes–Einstein relation yields a diffusion coefficient  $D = 32\ \mu\text{m}^2\text{ s}^{-1}$ . Our experimentally determined value is approximately 38% times higher than this value, which is still a satisfactory result. However, it is a little surprising that our result is higher than the value calculated from the Stokes–Einstein equation. Eq. (9) is an approximation [4], which is valid in the infinitely small stagnation point in the center of the cell, whereas an elliptical area of about  $1\text{ mm} \times 2\text{ mm}$  is probed in the experiments. Therefore we would expect a somewhat lower result. We compared our results with literature results obtained on silica particles by Böhmer et al. [6] and Hayes et al. [22]. Fig. 5 shows the diffusion coefficients as a function of the particle size. The literature data are indicated

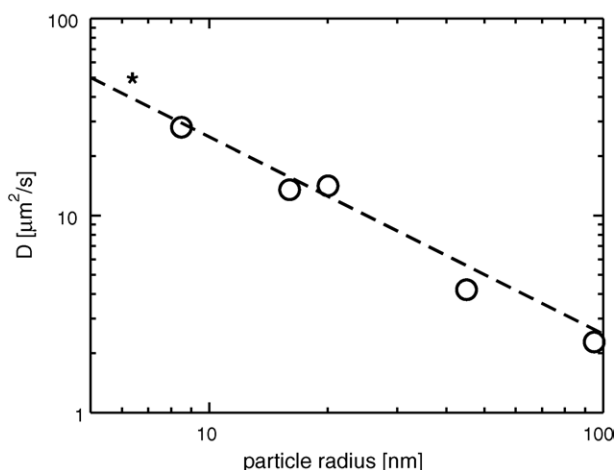


Fig. 5. Dependence of the diffusion coefficient on the particle size. The data from Böhmer and Hayes [6,22] are indicated with circles, our result with a star. The line is calculated using the Stokes–Einstein relation.

with circles, and our result is shown with a star. The Stokes–Einstein relation is indicated with a line. It is clear that our results are in good agreement with both literature data and the Stokes–Einstein relation. Secondly, we can conclude that the diffusion coefficient does not depend on the composition of the particles, which is to be expected since hydrodynamic drag is only determined by the particle geometry.

#### 4. Conclusions

The kinetics of irreversible deposition of gold nanocrystals from colloidal suspensions onto silicon/siliconoxide substrates is studied. Using a stagnation point flow geometry, the diffusive supply of colloidal particles is controlled. Simultaneously, the deposition process is monitored by in situ single wavelength reflectometry. The absolute coverage, calculated from the reflectometer signal by means of the thin island film theory, is measured as a function of time for different ionic strengths. Two regimes are distinguished, related to two different processes in the adsorption process. Initially, the deposition is merely governed by mass transport limited supply of colloidal particles, and the constant deposition rate is analyzed taking into account the cell geometry to obtain a diffusion coefficient for the nanocolloidal particles, which is slightly larger than what is calculated from the Stokes–Einstein relation. The ionic strength of the suspension only affects the deposition process in the saturation regime at higher coverages.

The coupling between the diffusion and the deposition process, i.e. the transition from mass transport limitation to the regime where surface blocking effects dominate, is analyzed using a generalized adsorption theory. In this theory, the deposition rate is expressed in terms of an overall kinetic blocking function. For the irreversible deposition of particles, the deposition is treated on the basis of the random sequential adsorption (RSA) model. For relatively large particles in the

<sup>2</sup> In fact, a dimensionless adsorption constant  $\bar{k}_a$  is given, which is related to the definition used here through  $\bar{k}_a = k_a \cdot \frac{L}{D}$  with  $L = (\pi a^2 c_0)^{-1}$  and  $D$  the diffusion coefficient.

micron range, RSA is directly applicable. For considerably smaller particles the aforementioned coupling is more pronounced. Using the generalized adsorption model, the measured deposition curves are adequately described, and the rate constant for particle adsorption is determined. Comparison with experimental results for proteins of similar dimensions as our colloidal particles, indicate that our results are in line with the adsorption rate constants for these proteins.

## References

- [1] H. Arwin, *Thin Solid Films* 313–314 (1998) 764.
- [2] G.J.M. Koper, *Colloids Surf. A* 165 (2000) 39.
- [3] E.S. Kooij, H. Wormeester, E.A.M. Brouwer, E. van Vroonhoven, A. van Silfhout, B. Poelsema, *Langmuir* 18 (2002) 4401.
- [4] Z. Adamczyk, B. Siwek, P. Warszyński, E. Musiał, *J. Colloid Interf. Sci.* 242 (2001) 14.
- [5] E.S. Kooij, E.A.M. Brouwer, H. Wormeester, B. Poelsema, *Langmuir* 18 (2002) 7677.
- [6] M.R. Böhm, E.A. van der Zeeuw, G.J.M. Koper, *J. Colloid Interf. Sci.* 197 (1998) 242.
- [7] Z. Adamczyk, M. Zembala, B. Siwek, P. Warszyński, *J. Colloid Interf. Sci.* 140 (1990) 123.
- [8] Z. Adamczyk, *Adv. Colloid Interf. Sci.* 100–102 (2003) 267.
- [9] Z. Adamczyk, *J. Colloid Interf. Sci.* 229 (2000) 477.
- [10] Z. Adamczyk, P. Weroński, *Adv. Colloid Interf. Sci.* 83 (1999) 137.
- [11] Z. Adamczyk, *Adsorption: Theory Modeling and Analysis*, Dekker, 2002 (Chapter 5).
- [12] E.A.M. Brouwer, E.S. Kooij, H. Wormeester, B. Poelsema, *Langmuir* 19 (2003) 8102.
- [13] J.C. Dijt, M.A. Cohen Stuart, J.E. Hofman, G.J. Fleer, *Colloids Surf. A* 51 (1990) 141.
- [14] H. Wormeester, E.S. Kooij, B. Poelsema, *Phys. Rev. B* 68 (2003) 085406.
- [15] D. Bedeaux, J. Vlieger, *Optical Properties of Surfaces*, Imperial College Press, London, 2002.
- [16] P. Schaaf, J. Talbot, *J. Chem. Phys.* 91 (1989) 4401.
- [17] P. Schaaf, J.-C. Voegel, B. Senger, *J. Phys. Chem. B* 104 (2000) 2204.
- [18] Z. Adamczyk, B. Senger, J.C. Voegel, P. Schaaf, *J. Chem. Phys.* 110 (1999) 3118.
- [19] J. Faraudo, J. Bafaluy, *J. Chem. Phys.* 112 (2000) 2003.
- [20] Z. Adamczyk, L. Szyk, *Langmuir* 16 (2000) 5730.
- [21] T. Dabros, T.G.M. van de Ven, *Colloid Polym. Sci.* 261 (1983) 694.
- [22] R.A. Hayes, M.R. Böhm, L.G.J. Fokink, *Langmuir* 15 (1999) 2865.